Skeletal Radiology
https://doi.org/10.1007/s00256-021-03823-7

REVIEW ARTICLE

Osteochondral lesions of the talar dome: an up-to-date approach to multimodality imaging and surgical techniques

Júlio Brandão Guimarães[1] · Isabela Azevedo Nicodemos da Cruz[1] · Caio Nery[2] · Flávio Duarte Silva[1] · Alípio Gomes Ormond Filho[1] · Bruno Cerretti Carneiro[1] · Marcelo Astolfi Caetano Nico[1]

Received: 13 January 2021 / Revised: 13 May 2021 / Accepted: 17 May 2021

Abstract

Osteochondral lesions (OCLs) of the talar dome consist of a multifactorial pathology of the articular cartilage and subchondral bone and can result in persistent ankle pain and osteoarthritis (OA). Along with a physical examination and clinical history, an imaging evaluation plays a pivotal role in the diagnosis of these lesions and is fundamental for making treatment decisions and determining prognosis by providing information regarding the size, location, and cartilage and subchondral bone statuses as well as associated lesions and degenerative changes. Multiple surgical techniques for OCLs of the talar dome have been developed in recent decades, including cartilage repair, regeneration, and replacement strategies, and radiologists should be acquainted with their specific expected and abnormal postoperative imaging findings to better monitor the results and predict poor outcomes. The present article proposes a thorough review of the ankle joint anatomy and biomechanics, physiopathology, diagnosis, and treatment of OCLs of the talar dome, highlighting the radiological approach and imaging findings in both pre- and postoperative scenarios.

Keywords Ankle joint · Talus · Cartilage · articular · Diagnostic imaging · Arthroscopy

Abbreviations

T1WI	T1-weighted imaging
T2WI	T2-weighted imaging
MRI	Magnetic resonance imaging
CR	Conventional radiography
CT	Computed tomography
OCL	Osteochondral lesion
BME	Bone marrow edema
BMS	Bone marrow stimulation
ACI	Autologous chondrocyte implantation
MACI	Matrix-induced autologous chondrocyte implantation
AMIC	Autologous matrix-induced chondrogenesis

✉ Isabela Azevedo Nicodemos da Cruz
isabela.cruz@grupofleury.com.br

Júlio Brandão Guimarães
julio.guimaraes@grupofleury.com.br

Caio Nery
caionerymd@gmail.com

Flávio Duarte Silva
flaviod.silva@grupofleury.com.br

Alípio Gomes Ormond Filho
alipio.ormond@grupofleury.com.br

Bruno Cerretti Carneiro
bruno.carneiro@grupofleury.com.br

Marcelo Astolfi Caetano Nico
marcelo.nico@grupofleury.com.br

[1] Department of Musculoskeletal Radiology, Fleury Medicina E Saúde Higienópolis, Rua Mato Grosso 306, 1st Floor, Higienópolis, São Paulo 01239-040, Brazil

[2] Department of Foot and Ankle Surgery, Federal University of São Paulo, Rua Napoleão de Barros 715, 1st Floor, Vila Clementino, São Paulo 04024-002, Brazil

Introduction

Osteochondral lesions (OCLs) of the talar dome consist of a multifactorial pathology that affects the articular cartilage and the subjacent subchondral bone. These lesions are associated with multiple etiologic factors, including acute trauma, repetitive microtrauma, vascularization deficits, biomechanical disturbances, systemic conditions, and genetic predisposition [1, 2]. Most talar OCLs are secondary to trauma, with a large number of ankle sprains resulting in some degree of osteochondral damage, especially if an ankle fracture is present, in which talar dome OCLs are

Published online: 15 June 2021

found in 61% of cases [3, 4]. The term *osteochondritis* dissecans (OCD) is usually reserved for a clinicopathological scenario of abnormal subchondral bone formation. This article reviews the particularities of the talus and the natural history, diagnosis, and treatment of OCLs of the talar dome, highlighting the role of imaging in this scenario.

Cartilage

The ankle cartilage presents characteristic anatomical, mechanical, and biochemical properties that make it unique. Highly congruent joints such as the tibiotalar joint present a sufficiently large area of contact to adequately distribute the load, which requires less cartilage deformation, unlike other less congruent joints, such as the knee [5]. Cartilage thickness is inversely related to joint congruence, with thin cartilage correlating with high congruence and a high compressive modulus [5]. The distal tibial plafond cartilage has a thickness ranging from 1.06 to 1.63 mm, and the talar dome has a thickness ranging from 0.94 to 1.62 mm, with a direct correlation with higher body mass index and male sex [6, 7]. The thickness of the talar dome also varies depending on the area, being thicker at the medial shoulder and thinner at the lateral gutter [6].

Ankle cartilage presents high dynamic stiffness, low permeability, and increased extracellular matrix density, providing resistance to load and mechanical damage. Compared to the knee cartilage, the ankle has a greater regenerative ability since its chondrocytes are less responsive to catabolic factors and more responsive to anabolic factors. The ankle cartilage also presents increased metabolism, translated into a lower half-life [8, 9].

Even though ankle osteoarthritis (OA) is rare, with a prevalence of 1%, posttraumatic OA accounts for more than 70% of cases, with advanced OA developing 20 years after the initial traumatic injury, impacting a patient's quality of life and burdening the health system [9].

Vascularization

Vascularization of the talus is unique: (a) almost two-thirds of the bone surface is covered in cartilage, (b) it presents no muscle or tendon attachment, and (c) irrigation of the talar dome is retrograde [10, 11]; all these features result in a limited arterial blood supply of the talar dome.

The vascular supply of the talus relies on the anterior tibial artery (36% of blood supply), posterior tibial artery (47%), and peroneal artery (17%), and the main contributor to the vascularization of the talar body is the anastomotic network between the artery of the tarsal canal (from the posterior tibial artery) and sinus tarsi artery within the bone [10] (Fig. 1a).

Lomax [12] studied the distribution of blood supply at the subchondral bone of the talar dome and showed that some areas are particularly less vascularized, especially the medial-equator, posterior medial, and posterior lateral sections. Importantly, these three sections are among the four most frequently affected in OCLs [12] (Fig. 1b).

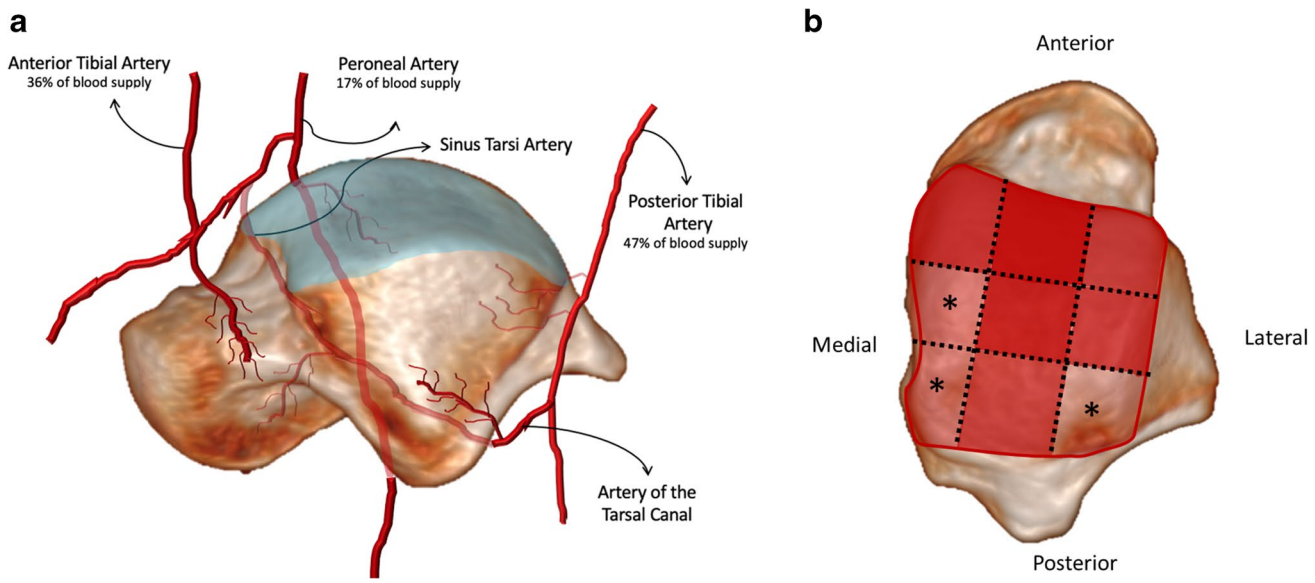

Fig. 1 Schematic representation of talar bone vascularization. **a** The vascular supply is unevenly distributed on the talar dome, and the least vascularized segments are medial-equator, medial-posterior, and lateral-posterior (asterisks). **b** The sections most frequently affected in OCLs

Biomechanics

The talar dome supports 4–5 times the body weight at heel rise during the stance phase of walking, which increases substantially during running. The force is mainly distributed by the tibiotalar joint, while only one-sixth is transmitted by talofibular articulation. Since the tibia is a longer bone, it can dissipate impact forces in a larger volume than the talus, which is a compact bone; therefore, OCLs are more common in the talar dome than in the tibial plafond [1, 13, 14].

The high congruence between the tibiofibular mortise and the talar trochlea promotes joint stability and improved force distribution. Minimal tilts or displacements reduce the contact area and therefore increase the zonal stress. Ramsey and Hamilton [15] and Lloyd et al. [16] studied the modification of the tibiotalar contact area with a lateral talar shift and showed that a 1-mm displacement leads to a 40–42% decrease in the contact area and shifts the stronger contact from anterior and lateral to posterior and medial. Bruns et al. [17] showed the modification of tibiotalar load distribution after ligament dissection, demonstrating a solid correlation between the degree of ligament rupture and pressure area and pressure maxima in different ankle positions.

Natural history of OCLs

Ankle sprains have an incidence of 2.15 per 1000 person-years in the USA [18]. The majority of OCLs of the talar dome are posttraumatic, and up to 6.5% of ankle sprains result in OCLs [19].

Traumatic stress consists mainly of axial load with ankle inversion, with impaction of the lateral border under dorsiflexion and of the medial border under plantar flexion and external rotation [3].

Following trauma, the main initial mechanism is cartilage injury due to shear stress. Trauma can cause chondral discontinuities that allow the insinuation of articular fluid into the site of the lesion, promoting osteolysis and the formation of subchondral cysts and resulting in progression of the chondral lesion itself [1]. High-impact trauma can also cause direct subchondral microfractures and bone impaction, hampering the support of the overlying cartilage by the subchondral bone and leading to instability of the cartilage/bone interface and consequent chondral lesions. Therefore, a cartilage lesion favors subchondral damage, and vice versa [1].

The established pathologic cycle translates clinically as deep ankle pain with or without swelling, which worsens with weight bearing and activity, with possible associated joint instability [1, 20].

If left untreated, OCLs can cause persistent pain in up to 14% of patients and limited daily or sports activities in approximately 23% and 58% of patients, respectively, with a low rate of progression to OA [21]. Some OCLs heal or remain inert and are asymptomatic, and complete regression of the lesion has been reported, especially in children [1, 21].

Diagnostic imaging

Conventional radiography (CR)

CR remains useful in the initial workup in acute ankle sprains or deep ankle pain with suspected OCLs of the talar dome, and the evaluation should include anteroposterior and lateral weight-bearing and mortise views [20]. Optional heel-rise views can improve the detection of OCLs. A routine radiological examination is unable to identify 30–50% of OCLs, especially if they are posteriorly located [22], but the combination of standard CR with a clinical history, physical examination, and mortise view with a 4.0-cm heel rise increases the sensitivity to 70% and specificity to 94% [19]. CR, however, is unsatisfactory for defining the location and extension of the lesions, both of which are pivotal factors for defining treatment and prognosis [19].

Computed tomography (CT)

The sensitivity and specificity of CT for the detection of OCLs are 81% and 99%, respectively [19]. CT with axial slices and a thickness of 0.6 mm and sagittal reformations of 1 mm is suggested [20]. Plantar flexion CT (patient in the supine position, with a slightly flexed knee and maximal plantar flexion, secured by a foot plate) can be performed in a preoperative scenario, especially in cases of posteriorly located OCLs and/or in ankles with a limited range of motion, and is a reliable and accurate method to evaluate whether a lesion can be assessed with an anterior arthroscopic approach [20, 23].

CT is the most accurate method to measure lesions and assess the subchondral bone plate, which plays an important role in the pathogenesis of OCLs [22]. The evaluation of the fragment and subchondral bone on CT has a good correlation with arthroscopic staging and helps predict cartilage damage [24]. The main limitations of this imaging method are radiation exposure and poor evaluation of the cartilage status, bone marrow edema (BME), and associated soft tissue lesions [20].

Magnetic resonance imaging (MRI)

MRI is the most appropriate method for the diagnosis of OCLs, with a sensitivity and specificity of 96% [19]. Even though the evaluation of ankle cartilage is challenging due to its small thickness, curvature, and articular congruence, MRI allows the identification of cartilage lesions and degeneration, especially with strong magnetic fields [25], sequence optimization, and dedicated/small field-of-view coils[26]. It also permits the visualization of BME, an important feature to be actively searched, especially in symptomatic patients. Even though MRI can overestimate the size of the lesion due to surrounding BME [19, 27], it can be used in routine practice.

Regarding ankle joint evaluations, 3.0-T MRI has been shown to be superior to 1.5-T MRI, as it has a higher signal-to-noise ratio and spatial resolution, resulting in a higher sensitivity in detecting cartilage, ligaments, and tendon pathology [28].

We propose an MR protocol that includes sagittal and axial T1- and T2FS-weighted images as well as a 3D coronal T2FS (Table 1). In our experience, the coronal volumetric sequence allows better evaluation of chondral lesions as well as of the bone plate. If 3D sequences are not feasible, we suggest either a coronal or sagittal plane with focus FOV and thin slices.

Advanced techniques can be performed with MRI, such as T2 mapping, T2* mapping, T1rho, and dGEMRIC, the last three of which are most relevant in scientific studies and have limited application in daily routine practice. T2 mapping, on the other hand, is more applicable in routine practice, as it does not require intravenous contrast injection and has been increasingly used in clinical practice in both pre- and postoperative scenarios. T2 mapping translates the biochemical modifications of the cartilage, permitting the identification of subtle changes that could be overlooked with conventional imaging and better characterizing the repair tissue after surgery, as shown in Fig. 2 [25].

Arthrography

Due to the low thickness of the articular cartilage and high congruence of the tibiotalar joint, the evaluation of cartilage defects can be challenging with conventional MR imaging. The use of intra-articular contrast may help to better delineate the cartilage surface and detect morphologic abnormalities. The high contrast and spatial resolution provided by CT arthrography (CTA) makes it a useful tool to detect chondral irregularities and discontinuities, with higher sensitivity, specificity, and interobserver agreement when compared to MRI for both partial- and full-thickness lesions [29]. However, it does not entail modification of treatment planning in most cases, lacks information on BME, and presents the drawbacks of an invasive method [29].

Compared to CTA, MR arthrography presents a far poorer delineation of the cartilage surface due to chemical shift artifacts, low spatial resolution, and lower contrast [30]. However, the sensitivities of MRA and CTA are fairly similar since the presence of BME indirectly indicates overlying chondral lesions and increases the reader's diagnostic performance [30].

Both methods are also useful to distinguish in situ stable and unstable OCLs, especially since conventional MRI still lacks accuracy for assessing fragment stability. The insinuation of contrast media underneath the osteochondral fragment indicates communication of intra-articular fluid with the interface between the lesion and its bed, showing instability [31], as shown in Fig. 3. CTA is especially more sensitive and specific than MRA for partially detached and detached in situ lesions, with higher interobserver agreement [32].

Table 2 summarizes the main information regarding diagnostic imaging for OCLs.

What to report?

Location

Medial lesions account for almost 62% of OCLs, lateral lesions account for approximately 36% of OCLs, and only 1% of OCLs occur in the center-third of the talar dome [2, 33]. Lateral lesions are most likely posttraumatic (94%), while only 64% of medial lesions present a history of previous trauma [34]. Lateral lesions are usually caused by shear stress and tend to be shallow and oval. On the other

Table 1 Suggested MR imaging protocol

Sequence	TR	TE	FOV	Thickness/gap	ETL	Matrix	NEX	Bandwidth
Sagittal T1	485	Min	15	4.0/0.4 mm	3	384×256	2	41.67
Sagittal T2 FS	2604	70	15	4.0/0.4 mm	20	256×224	4	41.67
Axial T1	595	Min	16	4.0/0.4 mm	3	352×192	1	31.25
Axial T2 FS	3823	60	16	4.0/0.4 mm	18	256×224	4	41.67
Coronal 3D T2FS	1300	84	16	0.6 mm/0	64	256×256	2	50
Coronal T2 map	900	8.1	14	3.0/0.6 mm		272×272	2	35.71

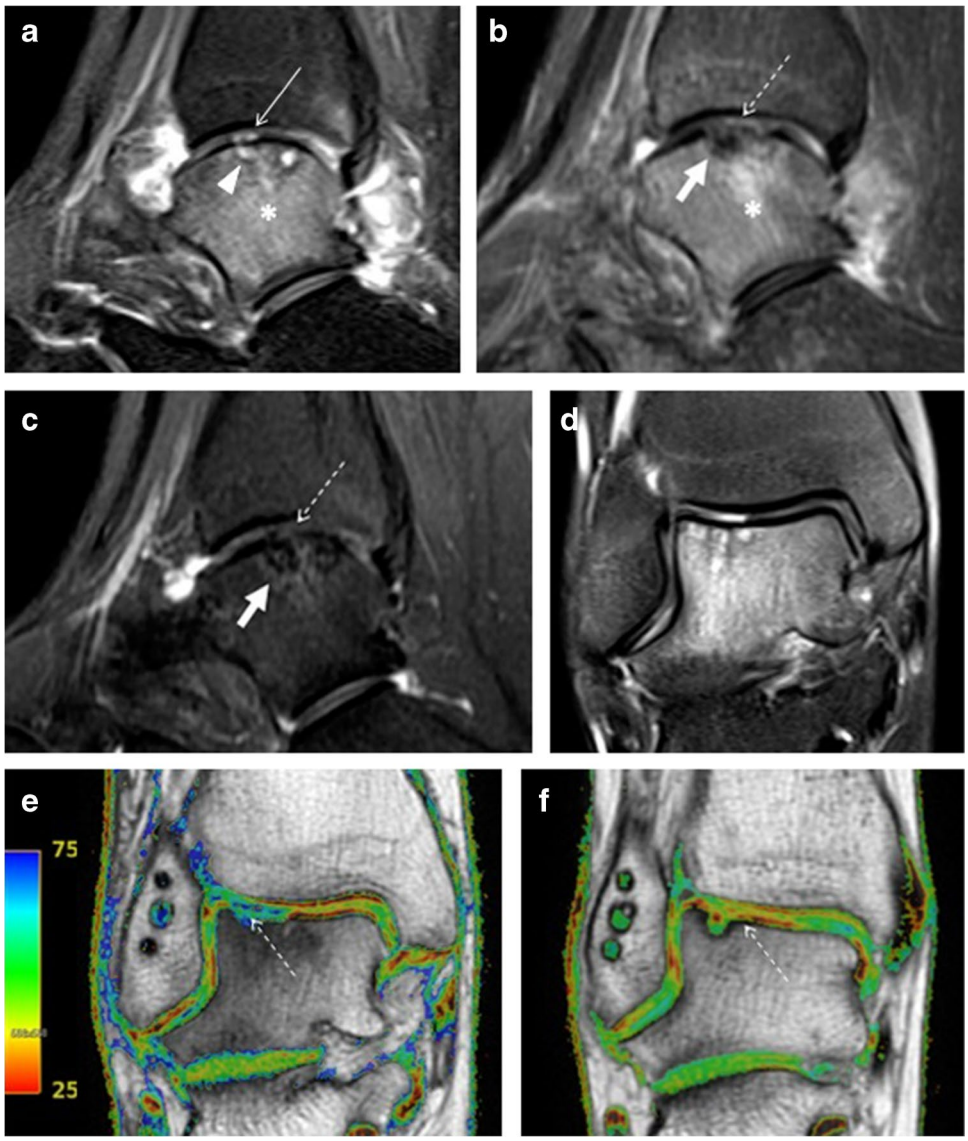

Fig. 2 Female, 19 years old, with a history of ankle sprain 10 months earlier. Preoperative MRI **a** and **b** demonstrates a chondral discontinuity (arrows), with an overall regular bone plate, but accompanied by subchondral bone cysts (arrowheads) and bone marrow edema (asterisk). The patient underwent bone marrow stimulation, and postoperative MRI performed 3 months after the surgery **c** and **d** shows partial resolution of the subchondral bone marrow edema (asterisk), sclerosis at the subchondral region (thick arrow), and mildly irregular reparative tissue (dashed arrow). One year later, a new MRI **e** and **f** shows good evolution of the same findings. On T2 mapping, note regular tissue covering the site of the OCL and the decrease in relaxation times over time, denoting the maturation of the reparative tissue **d** and **f**

hand, medial lesions usually occur due to torsional impaction and axial loading, resulting in deeper cup-shaped lesions [1, 2].

Raikin and Elias [2] proposed a 9-grid system to describe the location of lesions on the talar dome, dividing the talar dome surface into nine equally sized zones disposed in three columns (medial, central, and lateral) and three rows (anterior, equator, and posterior). They studied the frequency of OCLs in each area and showed that the medial-equator zone (53% of cases) and lateral-equator zone (25.7%) were the most affected by OCLs. Medial lesions were deeper and larger than lateral lesions [2]. When reporting the location of an OCL, the radiologist should use the 9-grid system and specify if the lesion extends to the shoulder of the talar dome when it is considered uncontained (Fig. 4).

Size

Since arthroscopic measurement of a lesion can be both inexact and challenging, the radiological approach is pivotal to assess the size of an OCL [20]. When reporting the size of an OCL, the radiologist should always measure the lesion in 3 planes (anteroposterior, laterolateral, and depth). MRI is frequently used in daily routine practice but may overestimate lesion size; therefore, for surgical planning, we suggest CT for precise measurements.

Cartilage status

As previously noted, the evaluation of ankle cartilage can be challenging with conventional MRI studies, but it is fundamental to guide treatment decisions. The Outerbridge

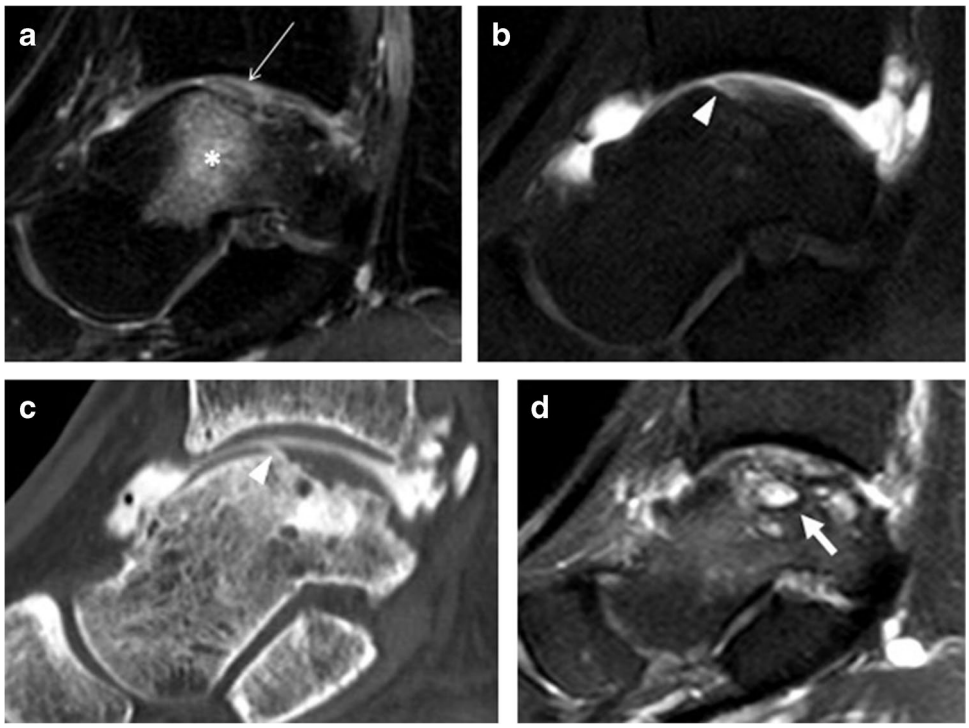

Fig. 3 A 24-year-old female with a history of ankle sprain was treated with matrix-augmented bone marrow stimulation with a collagen scaffold in 2012. Initial postoperative MRI **a** shows flattening and irregularity of the bone plane (white arrow) as well as bone marrow edema (asterisk) related to the surgical procedure. Six months later, the patient remained mildly symptomatic, and both arthro-MRI **b** and arthro-CT **c** were performed, showing the insinuation of contrast media underneath the anterior margin of the reparative tissue (arrowheads), which was more conspicuous in arthro-CT. Three years later, a new MRI was performed **d**, demonstrating the development of subchondral cysts (thick arrow), irregularities in the reparative tissue and osteophytes at the anterior tibiotalar margins, denoting poor evolution

classification [35] is an arthroscopic system first developed to stage cartilage lesions of the knee, and a correlation can be applied for imaging studies of the ankle as follows: grade 0, normal cartilage; grade 1, focal signal abnormalities; grade 2, surface irregularities or fraying; grade 3, partial thickness cartilage loss; and grade 4, subchondral bone exposed [36].

Subchondral bone changes

The subchondral bone is responsible for supporting the cartilage, influencing cartilage metabolism and distributing the load at the joint, and subchondral pathology is a source of pain in OCLs [24, 37].

Subchondral BME may translate a multifold of bone reactions, possibly representing an acute lesion, the deterioration of a chronic lesion, a reactive change to an increasingly unstable lesion, or a healing response [2, 26, 38]. Isolated BME with no major macroscopic chondral changes may represent occult cartilage injury, which can sometimes be identified only with arthroscopy [39]. If asymptomatic, BME associated with an OCL can be managed with conservative treatment [37]. However, if BME is progressive or associated with persistent pain, it may represent an unstable or progressive lesion.

The presence of subchondral bone cysts is an important feature that affects therapeutic decisions. They can result from initial trauma arising from microfractures in the subchondral plate that allow the penetration of joint fluid into the subchondral bone [26]; consequently, fluid pressure results in perfusion deficits, osteolysis, and cyst formation [1, 24]. Subchondral cysts are also considered a transient characteristic of OCL, representing a step of the pathological process and possibly healing with time [38]. They should be measured in their largest axis and indicated in the imaging report since the larger the cyst is, the less bone stock is available to support the bone plate and overlying cartilage.

After fluid pressure diminishes, bone remodeling starts and may result in sclerotic changes, which prevent spontaneous reintegration of the fragment and subjacent bone and should be reported [40]. When describing the subchondral bone changes of an OCL, the radiologist should report the presence of edema, subchondral cysts, and sclerosis. The length and depth of the subchondral cysts should be measured, and the subchondral bone loss should be evaluated, which are essential information for surgical planning.

Table 2 Diagnostic workup

Imaging method	Sensitivity/specificity	Advantages	Limitations	Particularities
Conventional radiography (CR)	0.59/0.91	Remains useful in the initial workup	Fails to detect up to 50% of OCLs	AP + lateral + AP mortise; heel rise increases sensitivity to 0.70
Computed tomography (CT)	0.81/0.99	Most accurate method to measure an OCL. Effective method to assess bone anatomy	Limited evaluation of the cartilage status, bone marrow edema, and soft tissue-associated lesions	Plantar flexion CT is useful for preoperative planning (especially in cases of posterior OCLs and/or ankles with limited range of motion)
Magnetic resonance imaging (MRI)	0.96/0.96	Assessment of the cartilage status, bone marrow edema, and soft tissue-associated lesions	May overestimate the size of the lesion	Advanced quantitative techniques may be used
Arthrograms	MRA 0.78–1.0/0.68–1.0 CTA 0.91–1.0/0.79–1.0	Useful to assess fragment stability and chondral discontinuities in doubtful cases	Invasive method; limited indications in routine practice	Even though arthro-MRI is useful due to additional information on soft tissues, arthro-CT is more useful due to high contrast and spatial resolution

Fragment status and stability

The status of any detached or displaced fragment should be assessed since fragment fixation can be a treatment option. The radiologist should report the largest diameter and thickness of the fragment, highlighting the bony thickness, since a minimal size and amount of bone are crucial to determine whether fixation is feasible [41]. To be considered for fixation, the fragment should be intact and viable [41], so its signal on MRI and the presence of sclerosis or fragmentation on CT should be evaluated.

Historically, the presence of a high signal line between an osteochondral fragment and the bed of the lesion is thought to represent the insinuation of synovial fluid behind the lesion, translating instability, which means that the lesion is not firmly attached to the subjacent bone and is unlikely to heal spontaneously [40, 42]. However, this line may also represent granulation tissue and, therefore, a healing response, with some of the lesions improving without a surgical approach [43, 44]. Unless there is a clear breach on the overlying cartilage, this sign should be interpreted carefully, as it may not be associated with an unstable lesion [44]. Moreover, a recent study by Nakasa et al. [40] aimed to correlate the intensity of the high signal line and the stability of the fragment by measuring the ratio between the T2 values of the joint fluid and the high signal line, and they concluded that the higher the signal of the line is, the more likely it represents fluid, denoting an unstable OCL.

In regular radiological reports, MRI has low accuracy (53%) for defining OCL stability, and even after the standardization of reports and application of specific classification systems, its accuracy increases to 76%, with low interreader agreement [45]. The evaluation of the lesion/underlying bone interface is limited with standard MRI protocols, devaluing the accurate assessment of stability [45].

Bohndorf [43] suggested the use of intravenous contrast to assess the high signal line at the lesion/bone interface since enhancement of the granulation tissue would distinguish it from insinuated joint fluid. Arthrograms are also useful in this scenario since the presence of contrast underneath the fragment represents communication with the joint space and is a sign of an unstable lesion.

Therefore, when describing the fragment status and stability of an OCL, the radiologist should measure the fragment and assess viability (assessment of bone marrow signal) and stability (evaluate the presence of fluid between the fragment and its bed).

Associated lesions and degenerative changes

Considering that OCLs of the talar dome are often posttraumatic and associated with ankle instability, it is important to report the status of the ligaments and the alignment of the hindfoot since the surgical approach may

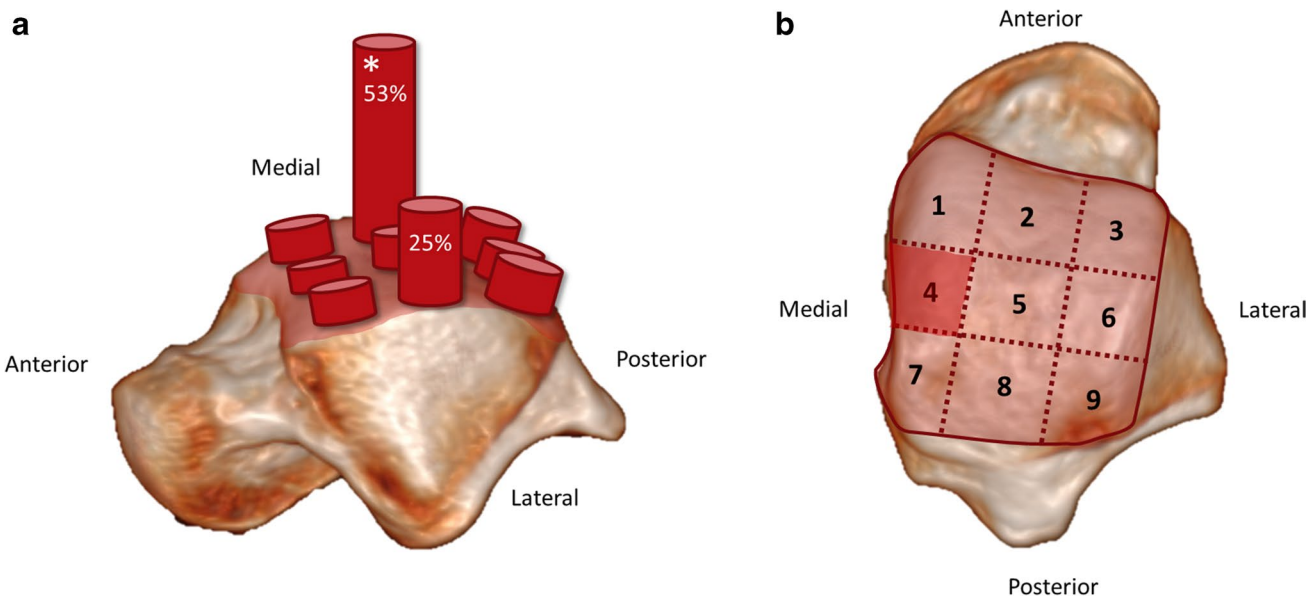

Fig. 4 Schematic representation of OCL distribution on the talar dome using the 9-grid system. Note that the medial equator zone is the most frequent site of OCLs and is also a poorly vascularized zone

also correct the malalignment and restore ankle stability [46]. The persistence of ankle instability is associated with a poor prognosis [47]. CR with axial load is useful to assess hindfoot alignment (varus/valgus, pes planus).

Ligamentous injuries, cartilage lesions of the tibial plafond, and degenerative abnormalities should be actively searched and reported, and these patients should undergo a prolonged follow-up since these findings are associated with negative outcomes and may contraindicate certain surgical approaches [41, 47].

The main information that should be reported when evaluating an OCL is summarized in Table 3.

Management

Treatment options for OCLs have greatly developed in recent decades, and new technologies and techniques have been used in this scenario. A revision of the main treatment options is described below, and Fig. 5 represents a simplified management algorithm.

Conservative treatment

In asymptomatic OCLs, surgical treatment is usually not required, and clinical and/or imaging examinations can be performed to follow its progression [3, 48]. Following acute trauma, symptomatic, nondisplaced OCLs can be managed with nonsurgical treatment, with a 4–6-week trial of immobilization and gradual return to normal activities [3, 48]. However, conservative treatment is effective in only approximately half of cases [33]. If osteoarthritic changes in the ankle are present, nonoperative treatment should be considered. Conservative treatment may also be considered for older patients with a low functional status or for patients with immature skeletal development [48]. In the absence of clinical recovery after 3 months, a new MRI scan should be

Table 3 What to report in the diagnostic evaluation of OCLs

Size	Measure in 3 planes; MRI is used in daily routine practice but may overestimate lesion size; for surgical planning, use CT for precise measurements
Location	Use the 9-grid system; specify if the lesion extends to the shoulder of the talar dome
Cartilage status	Evaluate cartilage signal, surface regularity, fissures, and/or erosions. Depth and length of abnormalities. Description is preferable to classification
Subchondral bone	Report the presence of edema, subchondral cysts, and sclerosis. Measure subchondral cysts and evaluate subchondral bone loss
Fragment	Measure and assess viability (assessment of bone marrow signal) and stability (evaluate the presence of fluid between the fragment and its bed)
Associated lesions	Ligament status, additional chondral defects, and degenerative abnormalities

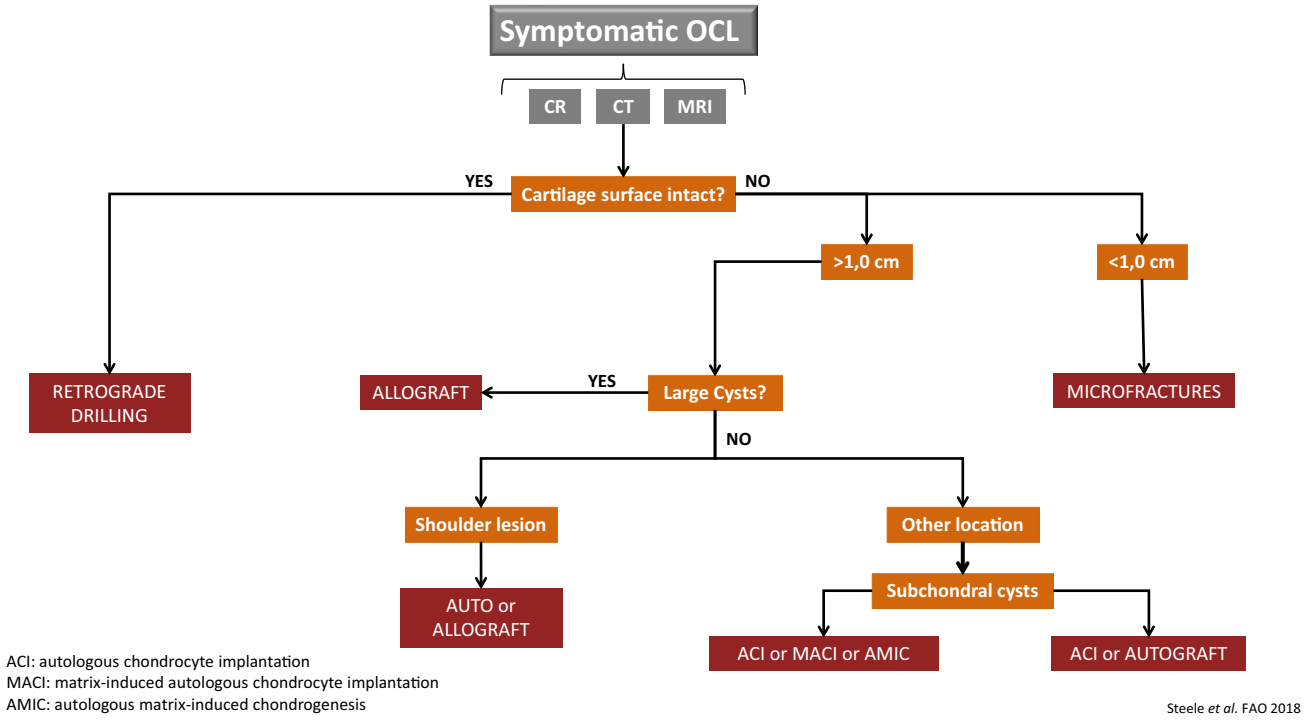

Fig. 5 Surgical management algorithm

performed, as the OCL is probably not healed and may have progressed [48].

Fixation

To preserve native cartilage and optimal congruence in the lesion, fixation of the osteochondral fragment may be indicated, with success rates ranging from 78 to 100% [41]. This technique can be performed in both acute and chronic scenarios for viable fragments larger than 1 cm and with a bone thickness of at least 3 mm [41, 49], preferably using two fixation devices.

Cartilage repair (bone marrow stimulation and retrograde drilling)

Bone marrow stimulation (BMS) is based on perforation of the subchondral bone, leading to local inflammatory reactions, the formation of fibrin clots, and the ingress of progenitor marrow cells [3, 50]. The defect is subsequently filled with fibrocartilage, which is composed of type I collagen, presents inferior mechanical properties to hyaline cartilage, and is likely to deteriorate over time [3, 51]. A systematic review by Ramponi et al. [51] showed that lesions larger than 107.4 mm^2 in area and 10.2 mm in diameter correlate with poor outcomes after BMS, indicating these sizes as thresholds up to which the fibrocartilage is able to endure biomechanical distress after the procedure. Overall, BMS has good results in pain and function in 65–90% of cases [3], as shown in Fig. 6, and almost 90% of athletic patients return to the preinjury level [51]; therefore, BMS remains the gold standard technique for lesions smaller than 10 m in diameter, 100 mm^2 in area, and 5 mm in depth [50]. The outcomes are worse in patients with underlying cysts, older lesions, or associated OA.

In cases with subchondral bone lesions or cysts with undamaged overlying cartilage, retrograde drilling can be performed (Fig. 7). It consists of a nonarticular procedure guided by arthroscopy and fluoroscopy, with the purpose of stimulating revascularization and bone formation at the subchondral bone while preserving overlying healthy cartilage [52]. A Kirschner wire is inserted from the posterolateral talus near the sinus tarsi to the subchondral defect to guide drilling and avoid damage to the cartilage. Over the wire, a drill is inserted to remove the necrotic bone and curette cystic material, followed by optional bone grafting [53, 54]. Success rates range between 81 and 100% and are especially advantageous for young patients due to higher bone-forming capacity than adults and avoidance of injury to the epiphyseal line [3, 33, 52, 55]. However, retrograde drilling should not be performed if the cartilage is damaged [3].

Fig. 6 Male, 8 years old, presented with deep ankle pain for 2 years that worsened after physical activities. Initial CR **a** shows an irregularity of the medial shoulder of the talar dome. MRI **b**, **c** was then performed, depicting an OCL at that location, with BME (asterisks) and mild subchondral plate impaction dashed arrow in **c**. On CT, there is a clear separation between the fragment and the lesion bed, consisting of a detached nondisplaced fragment thick arrow in **d**. Due to failed conservative treatment, the patient underwent fragment removal and microfractures **e** and **f**. Postoperative MRI shows repair tissue covering the site of the lesion (arrowheads) and postoperative changes and mild BME at the bed (curved arrow)

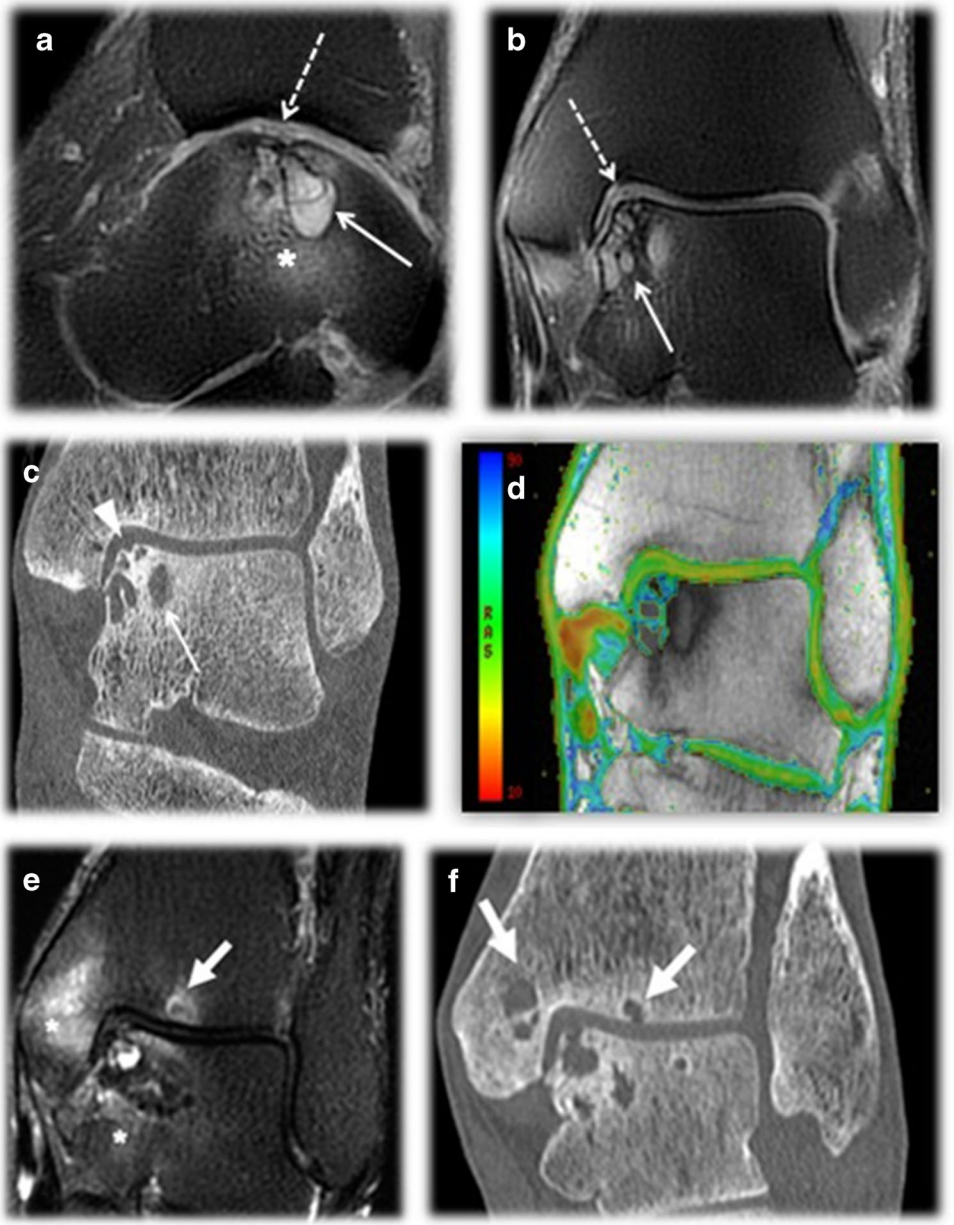

Fig. 7 Male, 63 years old, presented with a history of left ankle sprain while playing tennis 2 years prior and complained of deep ankle pain upon walking. MRI **a**, **b** and CT **c** show an OCL at the medial shoulder of the talar dome, with large cystic areas measuring 2.2 cm (white arrows) surrounded by BME asterisk in **a**. Note the irregularities of the subchondral bone plate (arrowhead in C) and minimal abnormalities of the cartilage surface, with no deep erosions (dashed arrows in **a** and **b**). T2 mapping revealed no significant modification in the relaxation time of the cartilage at the site of the lesion. Calcaneal osteotomy and retrograde drilling were performed. The patient's symptoms persisted, and MRI **e** and CT **f** performed 1 year after surgery reveal new subchondral cysts (thick arrows) and BME (asterisk) at the tibial plafond and medial malleolus, indicating poor evolution

Cartilage regeneration (scaffold-based therapy)

Autologous chondrocyte implantation (ACI) is a first-generation 2-step procedure consisting of the harvest of healthy cartilage (either from the anterior segment of the talus or from the knee) and chondrocyte culture, followed by second arthroscopy for the delivery of chondrocytes, which are then enclosed with an autologous periosteal membrane and fixed with sutures [3, 56]. The aim is to fill the osteochondral defect with mostly hyaline cartilage developed by implanted chondrocytes, with good postoperative results [3]. This procedure is indicated in OCLs larger than 1 cm^2, with or without cysts [56], with a success rate of 76% (70–92%) [33]. However, there are reservations about this technique due to periosteal hypertrophy [56].

Aiming to overcome the drawback of periosteal hypertrophy and to promote better distribution of chondrocytes at the site of the lesion, the matrix-induced autologous chondrocyte implantation (MACI) procedure was developed [3, 56]. This technique is a second-generation 2-step procedure consisting of the implantation of cultured chondrocytes in a scaffold, which is then inserted at the OCL site and fixed with fibrin glue, with good outcomes in 89% of cases [3, 56].

Both ACI and MACI require two surgical interventions, and to avoid this inconvenience, a single-stage scaffold-based procedure (autologous matrix-induced chondrogenesis, AMIC) was recently developed [3, 56]. Matrix-augmented bone marrow stimulation is a 1-step procedure

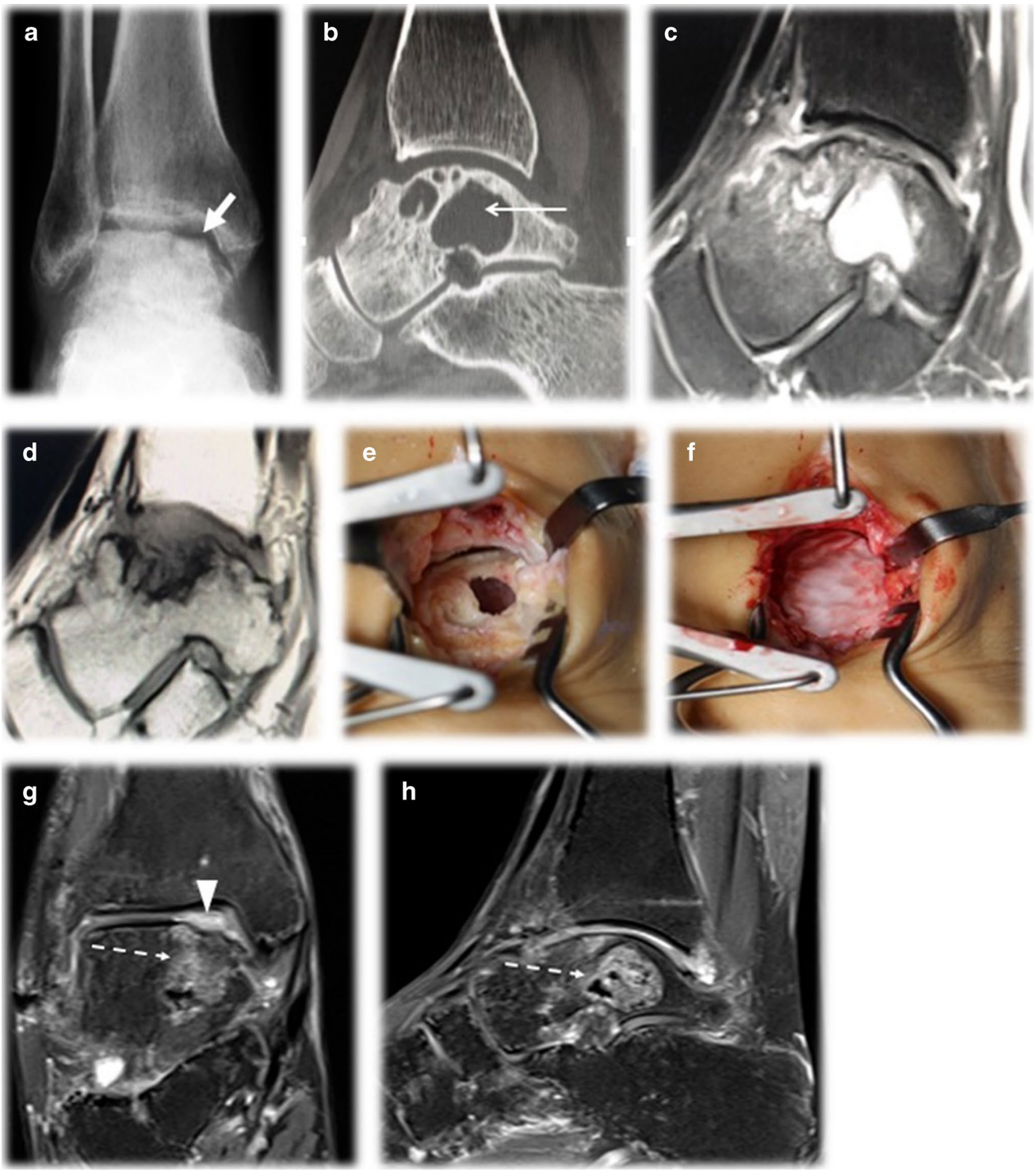

Fig. 8 A 42-year-old male presented with a history of chronic ankle instability, multiple previous sprains, and deep ankle pain for 5 years. CR **a** shows impaction and cortical irregularity at the medial shoulder of the talar dome (thick arrow). CT **b** and MRI **c** and **d** depict a large cystic OCL (arrows), with surrounding BME (asterisk). Note the important bone plate irregularity and impaction (dashed arrows). Surgery was performed **a**, **b**, with visualization of a large bone defect **e** filled with bone graft followed by implantation of a collagen membrane **f**. MRI **g** and **h** performed 2 months after surgery depicts satisfactory integration of the bone graft, with no significant BME (dashed arrows). The surface of the lesion is covered in high-signal tissue (arrowhead), which is expected in the early postoperative scenario

in which a collagen-matrix scaffold is placed over the lesion to support chondrogenic cells and blood clots that infiltrate the OCL after microfractures[46, 56, 57]. This procedure can be considered in lesions larger than 1 cm^2, if a single-step procedure is preferred or if bone grafting is necessary (in patients with more than 3-mm bone loss) [56], as shown in Fig. 8. Bone marrow aspirate concentrate (BMAc) or platelet-rich plasma (PRP) can be used to maximize chondrogenesis [3, 58]. Arthroscopic, clinical, and imaging outcomes are similar to those of ACI [3, 59], with successful results in pain reduction, ankle function, and return to sports [46].

Scaffold-based techniques should be considered in lesions larger than 1 cm^2 [56]. OCL size and location do not correlate with functional outcomes, and these procedures can be performed in both contained and uncontained lesions [56]. Scaffold-based therapy presents good long-term results since the repair tissue presents all components of hyaline cartilage and is very similar to native cartilage, in contrast to the shorter durability of the fibrocartilage formed after BMS [58] (Fig. 9).

Cartilage replacement (osteochondral autograft; osteochondral allograft; particulated juvenile cartilage allograft transplantation).

Osteochondral autografts are a technique based on the harvest of an autologous osteochondral plug to replace the OCL, with the advantage of restoring both the hyaline cartilage and subchondral bone with native material from the patient [3, 60]. The preferable donor site is the lateral femoral condyle, with less than 15% donor site morbidity [60]. Osteochondral autografts are generally indicated for cystic lesions larger than 1 cm and as a revision procedure after failed surgical treatment and can be considered in uncontained lesions, with satisfactory results [60]. Graft congruence is fundamental since a 1-mm proud graft increases pressure by 675% in lateral lesions and 255% in medial lesions [61]. Osteochondral autografts have good/excellent outcomes in over 85% of patients, with eventual poor outcomes [60, 62], as shown in Fig. 10.

Allograft implants can be considered to replace large defects for which other techniques may present poor results or if harvest of the plug from the patient's knee is not advisable [63]. This technique consists of replacement of the OCL by a graft removed from a fresh, nonfrozen talus of one from a cadaver donor [63]. Bulk osteochondral allografts should be considered in uncontained lesions or lesions larger than the size of 2 cylindrical osteochondral plugs, with improvement in ankle pain and function [63].

Postoperative imaging

It is important to standardize parameters to define posttreatment success for OCLs to better monitor the results and predict poor outcomes. The definition of success is clinical and consists of the absence of pain, patient satisfaction, return to work and sports, and an improvement of symptoms compared to pretreatment levels [47]. These data should be assessed at 3, 6, 12, and 24 months after treatment and annually thereafter [47].

The indication for a routine imaging evaluation after treatment consists of CR if the surgical approach includes bone graft or osteotomy to evaluate bone healing and integration, joint congruency, and assess hardware [47]. If the patient presents with symptoms or unsatisfactory functional outcomes, cross-sectional imaging can be performed, preferably with MRI, and Table 4 summarizes the main information that should be evaluated. Routine follow-up imaging in asymptomatic patients is not recommended [47].

As an attempt to homogenize the description of OCLs and standardize scientific studies, the MOCART system (MR Observation of Cartilage Repair Tissue – 2006) [64], initially described for the knee, has been used in ankle evaluations. While postoperative MRI provides valuable information regarding the structural integrity of the joint, the role of the MOCART score as a follow-up tool in cartilage repair of the ankle remains controversial (52).

The main information that should be described when evaluating posttreatment OCLs is defect filling, integration, status of repair tissue, subchondral bone, and associated complications. Table 4 describes in detail the key information that should be evaluated and reported.

Moreover, the radiologist should be acquainted with the surgical technique and consider its expected and abnormal specific findings when reading a postoperative study. Additionally, access to prior studies and close communications with the referring physician are essential.

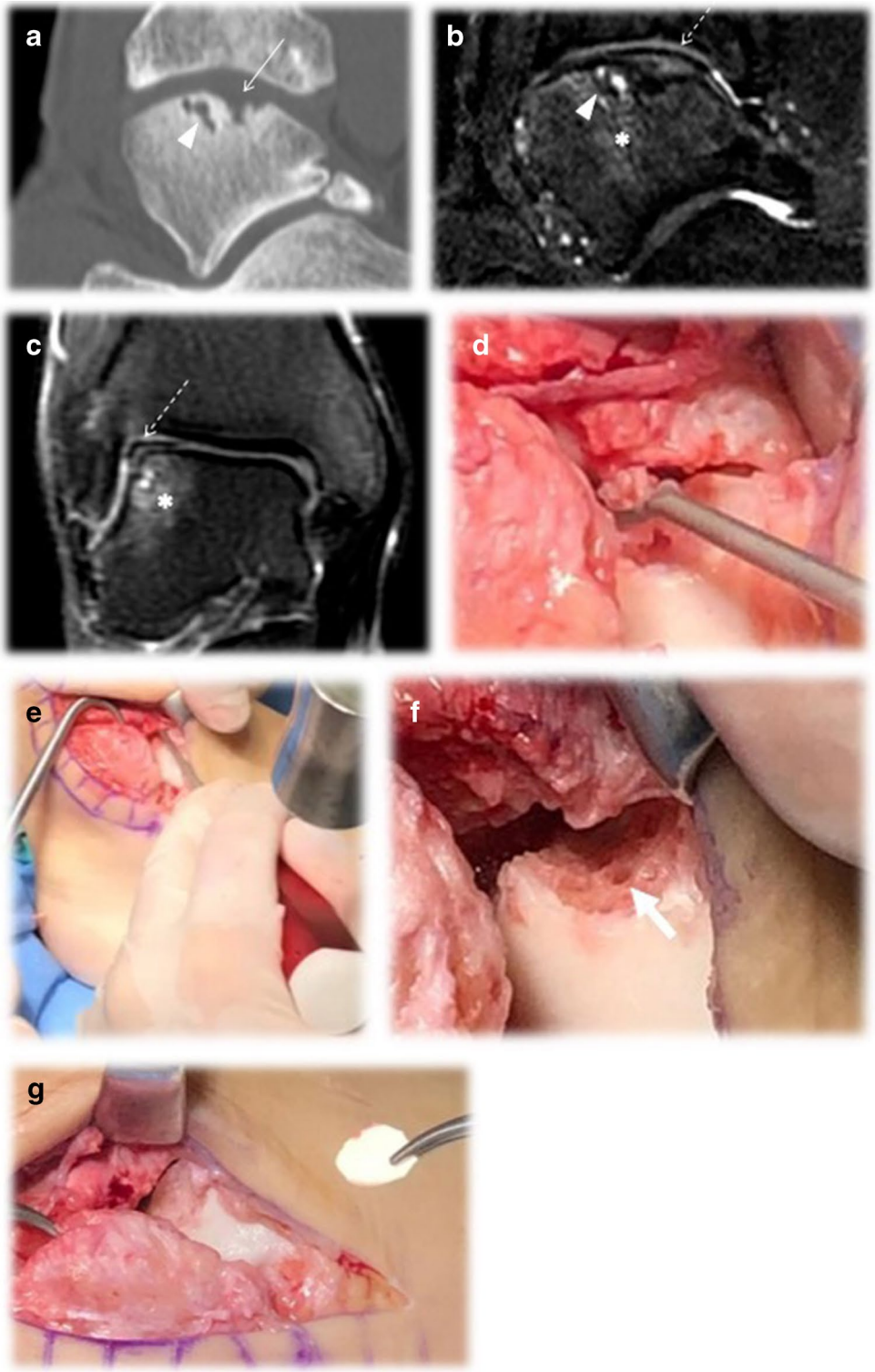

Fig. 9 Male, 28 years old, with a history of ankle sprain 3 years before, treated with microfractures 1 year later, with persistent deep ankle pain on sports activities. CT and MRI performed 2 years after bone marrow stimulation **a**, **b**, **c** depict irregularity and impaction of the subchondral bone plate (arrow), subchondral cysts (arrowheads) and bone marrow edema (asterisks). Note the hypertrophied fibrocartilage reparative tissue (dashed arrows). The patient underwent an open surgical procedure, with curettage of the lesion **a**, microfractures **b** and **c**, and placement of a collagen scaffold (matrix-augmented BMS)

Fig. 10 A 29-year-old male presented with a history of an acute ankle sprain with an OCL at the medial shoulder of the talar dome in 2007. The treatment of choice was autograft implantation. A few years after surgery **a**, **b**, the patient remained mildly symptomatic, and MRI shows subchondral plate irregularities and mild depression at the graft site (white arrows). The cartilage surface shows signal abnormalities and profound irregularities, with an uneven chondral surface (arrowheads). Three years later, the patient presented with worse deep ankle pain. MRI **c**-**e** depicts progression of the chondral lesion, with deep chondral erosions now also present in the adjacent tibial plafond (arrowheads). Note the progression of bone plate collapse as well as bone resorption surrounding the plug (dashed arrow in **e**). Bone marrow edema is pronounced (asterisks), and articular effusion is present. Considering the poor outcome of the autograft, the patient underwent hemiarthroplasty with the resurfacing technique 7 years after the first surgery, as shown on postoperative CT and CR **f**, **g**

Table 4 What to report on imaging follow-up

Defect filling	Volume and thickness: complete/partial filling; hypertrophy Surface regularity: regular/irregular
Integration	Bone integration: partial/complete integration with native bone Cartilage integration: partial/complete integration of reparative tissue with surrounding native cartilage
Status of repair tissue	Signal: homogeneous/heterogeneous; hyperintense/hypointense Fissures, flaps, or delaminations
Subchondral bone	Edema: compare with previous exams to evaluate progression or regression Cysts: compare with previous exams and measure
Associated complications	New chondral defects: both in talar dome or tibial plafond Effusion: regression is expected with time Osteoarthritis

Conclusion

Ankle sprains are a prevalent traumatic event, and a non-negligible proportion of these traumas are associated with OCLs of the talar dome. This pathology can result in persistent deep ankle pain and limited daily or sports activities and may progress to OA. CR, CT, and MRI each contribute important information regarding the OCL itself, associated lesions, and hindfoot alignment, highlighting the cardinal role of MRI in this pathology. Radiologists should be familiar with the imaging features of OCLs in both pre- and posttreatment scenarios as well as comprehend what to report to aid in orthopedists' management decisions and prevent patient morbidity.

Declarations

Conflict of interest The authors declare no competing interests.

References

1. van Dijk CN, Reilingh ML, Zengerink M, van Bergen CJ. Osteochondral defects in the ankle: why painful? Knee Surg Sports Traumatol Arthrosc. 2010;18(5):570–80.
2. Elias I, Zoga AC, Morrison WB, Besser MP, Schweitzer ME, Raikin SM. Osteochondral lesions of the talus: localization and morphologic data from 424 patients using a novel anatomical grid scheme. Foot Ankle Int. 2007;28(2):154–61.
3. Steele J, Dekker T, Federer A, Liles J, Adams S, Easley M. Osteochondral lesions of the talus: current concepts in diagnosis and treatment. Foot & Ankle Orthopaedics. 2018;3:247301141877955.
4. Leontaritis N, Hinojosa L, Panchbhavi VK. Arthroscopically detected intra-articular lesions associated with acute ankle fractures. J Bone Joint Surg Am. 2009;91(2):333–9.
5. Sophia Fox AJ, Bedi A, Rodeo SA. The basic science of articular cartilage: structure, composition, and function. Sports Health. 2009;1(6):461–8.
6. Sugimoto K, Takakura Y, Tohno Y, Kumai T, Kawate K, Kadono K. Cartilage thickness of the talar dome. Arthroscopy. 2005;21(4):401–4.
7. Shepherd DE, Seedhom BB. Thickness of human articular cartilage in joints of the lower limb. Ann Rheum Dis. 1999;58(1):27–34.
8. Kuettner KE, Cole AA. Cartilage degeneration in different human joints. Osteoarthr Cartil. 2005;13(2):93–103.
9. Kraeutler MJ, Kaenkumchorn T, Pascual-Garrido C, Wimmer MA, Chubinskaya S. Peculiarities in ankle cartilage. Cartilage. 2017;8(1):12–8.
10. Miller AN, Prasarn ML, Dyke JP, Helfet DL, Lorich DG. Quantitative assessment of the vascularity of the talus with gadolinium-enhanced magnetic resonance imaging. J Bone Joint Surg Am. 2011;93(12):1116–21.
11. Melenevsky Y, Mackey RA, Abrahams RB, Thomson NB. Talar fractures and dislocations: a radiologist's guide to timely diagnosis and classification. Radiographics. 2015;35(3):765–79.
12. Lomax A, Miller RJ, Fogg QA, Jane Madeley N, Senthil KC. Quantitative assessment of the subchondral vascularity of the talar dome: a cadaveric study. Foot Ankle Surg. 2014;20(1):57–60.
13. Procter P, Paul JP. Ankle joint biomechanics. J Biomech. 1982;15(9):627–34.
14. Mow V, Flatow E, Ateshian G. Biomechanics. In: SR S, editor. Orthopaedic basic science: biology and biomechanics of the musculoskeletal system. 2nd ed. Rosemont, US: American Academy Orthopedic Surgeons 2000. p. 133–80.
15. Ramsey PL, Hamilton W. Changes in tibiotalar area of contact caused by lateral talar shift. J Bone Joint Surg Am. 1976;58(3):356–7.
16. Lloyd J, Elsayed S, Hariharan K, Tanaka H. Revisiting the concept of talar shift in ankle fractures. Foot Ankle Int. 2006;27(10):793–6.
17. Bruns J, Rosenbach B. Pressure distribution at the ankle joint. Clin Biomech (Bristol, Avon). 1990;5(3):153–61.
18. Waterman BR, Owens BD, Davey S, Zacchilli MA, Belmont PJ. The epidemiology of ankle sprains in the United States. J Bone Joint Surg Am. 2010;92(13):2279–84.
19. Verhagen RA, Maas M, Dijkgraaf MG, Tol JL, Krips R, van Dijk CN. Prospective study on diagnostic strategies in osteochondral lesions of the talus. Is MRI superior to helical CT? J Bone Joint Surg Br. 2005;87(1):41–6.
20. van Bergen CJA, Baur OL, Murawski CD, Spennacchio P, Carreira DS, Kearns SR, et al. Diagnosis: history, physical examination, imaging, and arthroscopy: Proceedings of the International Consensus Meeting on Cartilage Repair of the Ankle. Foot Ankle Int. 2018;39(1_suppl):3S-8S.
21. Klammer G, Maquieira GJ, Spahn S, Vigfusson V, Zanetti M, Espinosa N. Natural history of nonoperatively treated osteochondral lesions of the talus. Foot Ankle Int. 2015;36(1):24–31.

22. van Bergen CJ, Gerards RM, Opdam KT, Terra MP, Kerkhoffs GM. Diagnosing, planning and evaluating osteochondral ankle defects with imaging modalities. World J Orthop. 2015;6(11):944–53.
23. van Bergen CJ, Tuijthof GJ, Blankevoort L, Maas M, Kerkhoffs GM, van Dijk CN. Computed tomography of the ankle in full plantar flexion: a reliable method for preoperative planning of arthroscopic access to osteochondral defects of the talus. Arthroscopy. 2012;28(7):985–92.
24. Nakasa T, Adachi N, Kato T, Ochi M. Appearance of subchondral bone in computed tomography is related to cartilage damage in osteochondral lesions of the talar dome. Foot Ankle Int. 2014;35(6):600–6.
25. Schreiner MM, Mlynarik V, Zbýň Š, Szomolanyi P, Apprich S, Windhager R, et al. New technology in imaging cartilage of the ankle. Cartilage. 2017;8(1):31–41.
26. Griffith JF, Lau DT, Yeung DK, Wong MW. High-resolution MR imaging of talar osteochondral lesions with new classification. Skeletal Radiol. 2012;41(4):387–99.
27. Yasui Y, Hannon CP, Fraser EJ, Ackermann J, Boakye L, Ross KA, et al. Lesion size measured on MRI does not accurately reflect arthroscopic measurement in talar osteochondral lesions. Orthop J Sports Med. 2019;7(2):2325967118825261.
28. Barr C, Bauer JS, Malfair D, Ma B, Henning TD, Steinbach L, et al. MR imaging of the ankle at 3 Tesla and 1.5 Tesla: protocol optimization and application to cartilage, ligament and tendon pathology in cadaver specimens. Eur Radiol. 2007;17(6):1518–28.
29. Kirschke JS, Braun S, Baum T, Holwein C, Schaeffeler C, Imhoff AB, et al. Diagnostic value of CT arthrography for evaluation of osteochondral lesions at the ankle. Biomed Res Int. 2016;2016:3594253.
30. Schmid MR, Pfirrmann CW, Hodler J, Vienne P, Zanetti M. Cartilage lesions in the ankle joint: comparison of MR arthrography and CT arthrography. Skeletal Radiol. 2003;32(5):259–65.
31. Cerezal L, Abascal F, García-Valtuille R, Canga A. Ankle MR arthrography: how, why, when. Radiol Clin North Am. 2005;43(4):693–707, viii.
32. Pirimoglu B, Ogul H, Polat G, Kantarci M, Levent A. The comparison of direct magnetic resonance arthrography with volumetric interpolated breath-hold examination sequence and multidetector computed tomography arthrography techniques in detection of talar osteochondral lesions. Acta Orthop Traumatol Turc. 2019;53(3):209–14.
33. Zengerink M, Struijs PA, Tol JL, van Dijk CN. Treatment of osteochondral lesions of the talus: a systematic review. Knee Surg Sports Traumatol Arthrosc. 2010;18(2):238–46.
34. Tol JL, Struijs PA, Bossuyt PM, Verhagen RA, van Dijk CN. Treatment strategies in osteochondral defects of the talar dome: a systematic review. Foot Ankle Int. 2000;21(2):119–26.
35. OUTERBRIDGE RE. The etiology of chondromalacia patellae. J Bone Joint Surg Br. 1961;43-B:752–7.
36. Posadzy M, Desimpel J, Vanhoenacker F. Staging of osteochondral lesions of the talus: MRI and cone beam CT. J Belg Soc Radiol. 2017;101(Suppl 2):1.
37. Shimozono Y, Brown AJ, Batista JP, Murawski CD, Gomaa M, Kong SW, et al. Subchondral pathology: Proceedings of the International Consensus Meeting on Cartilage Repair of the Ankle. Foot Ankle Int. 2018;39(1_suppl):48S-53S.
38. Elias I, Jung JW, Raikin SM, Schweitzer MW, Carrino JA, Morrison WB. Osteochondral lesions of the talus: change in MRI findings over time in talar lesions without operative intervention and implications for staging systems. Foot Ankle Int. 2006;27(3):157–66.
39. Forney M, Subhas N, Donley B, Winalski CS. MR imaging of the articular cartilage of the knee and ankle. Magn Reson Imaging Clin N Am. 2011;19(2):379–405.
40. Nakasa T, Ikuta Y, Ota Y, Kanemitsu M, Sumii J, Nekomoto A, et al. Relationship of T2 Value of high-signal line on MRI to the fragment in osteochondral lesion of the talus. Foot Ankle Int. 2020;41(6):698–704.
41. Reilingh ML, Murawski CD, DiGiovanni CW, Dahmen J, Ferrao PNF, Lambers KTA, et al. Fixation techniques: Proceedings of the International Consensus Meeting on Cartilage Repair of the Ankle. Foot Ankle Int. 2018;39(1_suppl):23S-7S.
42. De Smet AA, Ilahi OA, Graf BK. Reassessment of the MR criteria for stability of osteochondritis dissecans in the knee and ankle. Skeletal Radiol. 1996;25(2):159–63.
43. Bohndorf K. Osteochondritis (osteochondrosis) dissecans: a review and new MRI classification. Eur Radiol. 1998;8(1):103–12.
44. O'Connor MA, Palaniappan M, Khan N, Bruce CE. Osteochondritis dissecans of the knee in children. A comparison of MRI and arthroscopic findings. J Bone Joint Surg Br. 2002;84(2):258–62.
45. Ellermann JM, Donald B, Rohr S, Takahashi T, Tompkins M, Nelson B, et al. Magnetic resonance imaging of osteochondritis dissecans: validation study for the ICRS Classification System. Acad Radiol. 2016;23(6):724–9.
46. Weigelt L, Hartmann R, Pfirrmann C, Espinosa N, Wirth SH. Autologous matrix-induced chondrogenesis for osteochondral lesions of the talus: a clinical and radiological 2- to 8-year follow-up study. Am J Sports Med. 2019;47(7):1679–86.
47. van Dijk PAD, Murawski CD, Hunt KJ, Andrews CL, Longo UG, McCollum G, et al. Post-treatment follow-up, imaging, and outcome scores: Proceedings of the International Consensus Meeting on Cartilage Repair of the Ankle. Foot Ankle Int. 2018;39(1_suppl):68S-73S.
48. Dombrowski ME, Yasui Y, Murawski CD, Fortier LA, Giza E, Haleem AM, et al. Conservative management and biological treatment strategies: Proceedings of the International Consensus Meeting on Cartilage Repair of the Ankle. Foot Ankle Int. 2018;39(1_suppl):9S-15S.
49. Nakasa T, Ikuta Y, Ota Y, Kanemitsu M, Adachi N. Clinical Results of bioabsorbable pin fixation relative to the bone condition for osteochondral lesion of the talus. Foot Ankle Int. 2019;40(12):1388–96.
50. Hannon CP, Bayer S, Murawski CD, Canata GL, Clanton TO, Haverkamp D, et al. Debridement, curettage, and bone marrow stimulation: Proceedings of the International Consensus Meeting on Cartilage Repair of the Ankle. Foot Ankle Int. 2018;39(1_suppl):16S-22S.
51. Ramponi L, Yasui Y, Murawski CD, Ferkel RD, DiGiovanni CW, Kerkhoffs GMMJ, et al. Lesion Size is a predictor of clinical outcomes after bone marrow stimulation for osteochondral lesions of the talus: a systematic review. Am J Sports Med. 2017;45(7):1698–705.
52. Ikuta Y, Nakasa T, Ota Y, Kanemitsu M, Sumii J, Nekomoto A, et al. Retrograde drilling for osteochondral lesion of the talus in juvenile patients. Foot & Ankle Orthopaedics. 2020;5(2):2473011420916139.
53. Jimeno Torres E, Ibañez M, Campillo Recio D, Alberti Fito G, Mendez Gil A, Jimeno Torres JM. Retrograde drilling with tibial autograft in osteochondral lesions of the talar dome. Arthrosc Tech. 2020;9(8):e1155–61.
54. Hyer CF, Berlet GC, Philbin TM, Lee TH. Retrograde drilling of osteochondral lesions of the talus. Foot Ankle Spec. 2008;1(4):207–9.
55. Minokawa S, Yoshimura I, Kanazawa K, Hagio T, Nagatomo M, Sugino Y, et al. Retrograde drilling for osteochondral lesions of the talus in skeletally immature children. Foot Ankle Int. 2020;41(7):827–33.
56. Rothrauff BB, Murawski CD, Angthong C, Becher C, Nehrer S, Niemeyer P, et al. Scaffold-based therapies: Proceedings of the International Consensus Meeting on Cartilage Repair of the Ankle. Foot Ankle Int. 2018;39(1_suppl):41S-7S.

57. Yasui Y, Wollstein A, Murawski CD, Kennedy JG. Operative treatment for osteochondral lesions of the talus: biologics and scaffold-based therapy. Cartilage. 2017;8(1):42–9.
58. Giannini S, Buda R, Cavallo M, Ruffilli A, Cenacchi A, Cavallo C, et al. Cartilage repair evolution in post-traumatic osteochondral lesions of the talus: from open field autologous chondrocyte to bone-marrow-derived cells transplantation. Injury. 2010;41(11):1196–203.
59. Giannini S, Buda R, Battaglia M, Cavallo M, Ruffilli A, Ramponi L, et al. One-step repair in talar osteochondral lesions: 4-year clinical results and T2-mapping capability in outcome prediction. Am J Sports Med. 2013;41(3):511–8.
60. Hurley ET, Murawski CD, Paul J, Marangon A, Prado MP, Xu X, et al. Osteochondral autograft: Proceedings of the International Consensus Meeting on Cartilage Repair of the Ankle. Foot Ankle Int. 2018;39(1_suppl):28S-34S.
61. Latt LD, Glisson RR, Montijo HE, Usuelli FG, Easley ME. Effect of graft height mismatch on contact pressures with osteochondral grafting of the talus. Am J Sports Med. 2011;39(12):2662–9.
62. Shimozono Y, Hurley ET, Myerson CL, Kennedy JG. Good clinical and functional outcomes at mid-term following autologous osteochondral transplantation for osteochondral lesions of the talus. Knee Surg Sports Traumatol Arthrosc. 2018;26(10):3055–62.
63. Smyth NA, Murawski CD, Adams SB, Berlet GC, Buda R, Labib SA, et al. Osteochondral allograft: Proceedings of the International Consensus Meeting on Cartilage Repair of the Ankle. Foot Ankle Int. 2018;39(1_suppl):35S-40S.
64. Marlovits S, Singer P, Zeller P, Mandl I, Haller J, Trattnig S. Magnetic resonance observation of cartilage repair tissue (MOCART) for the evaluation of autologous chondrocyte transplantation: determination of interobserver variability and correlation to clinical outcome after 2 years. Eur J Radiol. 2006;57(1):16–23.